Progress In Electromagnetics Research, Vol. 141, 431–441, 2013

STUDY OF HIGH EFFICIENCY NOVEL FOLDED WAVEGUIDE TRAVELING-WAVE TUBE WITH SHEET ELECTRON BEAM

Yan Hou*, Jin Xu, Shao-Meng Wang, Zhi-Gang Lu, Yan-Yu Wei, and Yu-Bin Gong

National Key Laboratory of Science and Technology on Vacuum Electronics, School of Physical Electronics, University of Electronic Science and Technology of China, Chengdu 610054, China

Abstract—A novel double-ridge loaded folded waveguide (FWG) traveling-wave tube (TWT) amplifier for sheet electron beam working at 140 GHz is proposed in this paper. The dispersion relation and interaction impedance characteristics have been analyzed based on the equivalent circuit method. The transmission properties and nonlinear interaction are investigated. The simulation results reveal that the double-ridge loaded FWG-TWT with sheet electron beam can make full use of relatively large electronic fields, and the average output power can be over 110 W at 140 GHz when the electron beam voltage and the current of the sheet beam are set to 12.7 kV and 150 mA, respectively. Meanwhile, the maximum gain and interaction efficiency can reach 34 dB and 12%, respectively. Compared with the traditional FWG-TWT, the novel FWG-TWT has the advantages of much higher efficiency and bigger output power.

1. INTRODUCTION

Realization of the fully-integrated high power millimeter-wave amplifiers with moderate bandwidth will have significant impact on a variety of defense applications, such as high data-rate communication, airborne collision avoidance systems, and high resolution radar imaging. These amplifiers require robust all-metal structures for thermal handling capability, which limits the use of conventional wide-band traveling-wave tubes (TWTs), such as the helix. The folded-waveguide (FWG) circuit [1–7] can be chosen as a compromise between

Received 5 June 2013, Accepted 20 July 2013, Scheduled 26 July 2013

* Corresponding author: Yan Hou (houyan0308@163.com).

the wide bandwidth of the helix and the high power handling the coupled-cavity structure. Based on previous investigation results of the FWG-TWT [8–11], a lot of considerable efforts have been devoted to exploring novel structures to improve the performance of tube [12–15]. On the other hand, as the energy source in the TWT is the electron beam that emits from a thermionic cathode, the power is limited by maximum current density. The sheet electron beam [16] has become more interesting than the conventional pencil electron beam because of its lager current transport capacity, relatively lower space charge effect and possessing larger power capacity.

In order to get higher output power of the TWT at 140 GHz, we designed a novel broadband double-ridge loaded FWG-TWT with sheet electron beam. The ultimate goal of our research was to develop a 140 GHz FWG-TWT with broadband, high beam-wave energy conversion efficiency and relatively high output power. Based on the cold-circuit calculation results by means of equivalent circuit in this paper, we constructed full 3-D beam-wave interaction circuit model. Furthermore, the CST Studio Suites [17] were carried out to predict and optimize the performance of the double-ridge loaded FWG slow wave structure (SWS).

2. DOUBLE-RIDGE LOADED SLOW-WAVE STRUCTURE

This kind of slow wave structure is shown in Figure 1, which is evolved from the original serpentine FWG-SWS, and combined with the advantages of the traditional FWG-SWS, *E*-plane loaded FWG-SWS and *H*-plane loaded FWG-SWS. In this structure, the wide and narrow sides of the straight portions of the traditional FWG-SWS have been changed because of the double ridge loaded. A sheet electron beam tunnel passes through the *E*-plane of straight portions of the double-ridge loaded FWG-SWS.

The fundamental mode TE10 of the rectangular waveguide is a symmetrical mode, which is the operation mode in the double-ridge loaded FWG-TWT as shown in Figure 2. A sinusoidal phase variation along the axial direction is observed. The red color represents the positive direction of the longitudinal electric fields, and the blue one represents the negative direction. It means that the accelerating and retarding electronic fields distribute periodically along the axial direction, which is the requirements for amplification mechanism of the TWT.

As can been seen in Figure 2 which is obtained from the CST-PS 3-D particle-in-cell simulation, the electric field is mainly distributed in

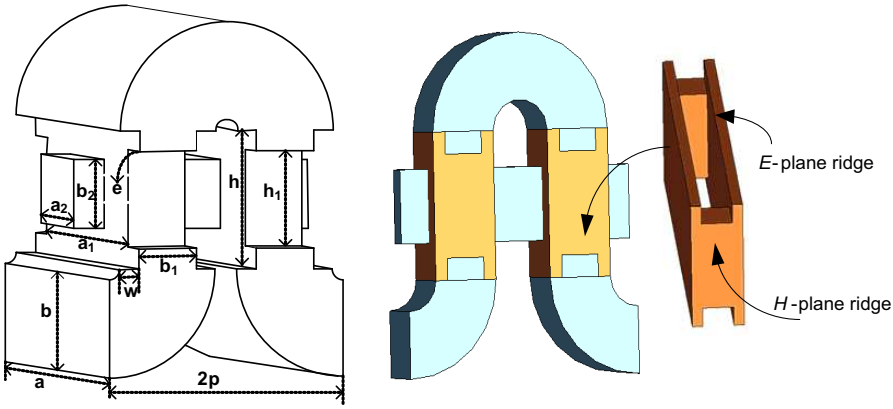

(a) (b)

Figure 1. (a) Dimensional parameters of double-ridge loaded FWG-SWS; (b) the model of E-plane and H-plane loaded FWG-SWS.

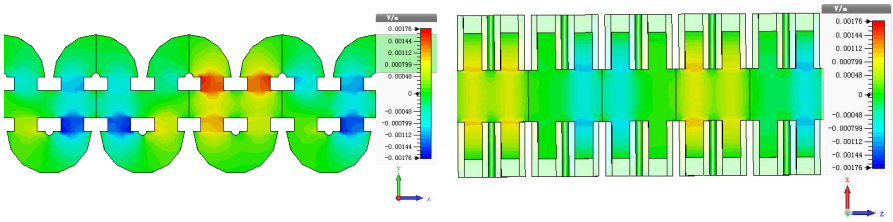

(a) (b)

Figure 2. Longitudinal component of electric field distribution of the fundamental mode on (a) H-plane and (b) E-plane of the double-ridge loaded FWG-SWS.

the middle of the broad side of rectangular waveguide, and the closer to the side wall, the weaker the electric field becomes. Therefore, the traditional pencil beam tunnel covers smaller area than that of the sheet beam, so that the relatively strong electric field beyond the beam channel could not be fully utilized in the beam-wave interaction, and the improvement of the output power is thereby limited. In order to select appropriate parameter of the sheet beam tunnel, we have done some preliminary analysis of the longitudinal electric field distribution in the transverse direction. These results are given in the Figures 3 and 4. In fact, the field distribution should be symmetric in both x and y directions. However, due to the numerical error in the process of our calculation, the field distributions of the double-ridge loaded FWG-SWS are not exactly symmetric.

The horizontal axis represents the distance from the observation point to the center on the broad wall of the double-ridge loaded SWS. The left and right vertical axes represent the amplitude of electric field and interaction impedance, respectively. It is observed from the Figure 3 that the maximum values for the longitudinal electric field and interaction impedance appear in the center of the channel, while at the edge of the broad wall, both electric fields and interaction impedance may be zero. But considering the effects of beam the tunnel, the electric fields and interaction impedance distribution are depicted in Figure 4. It is indicated that both electric fields and interaction impedance are minimum in the middle, while the maximum electric fields and interaction impedance appear at observation point 0.3 mm

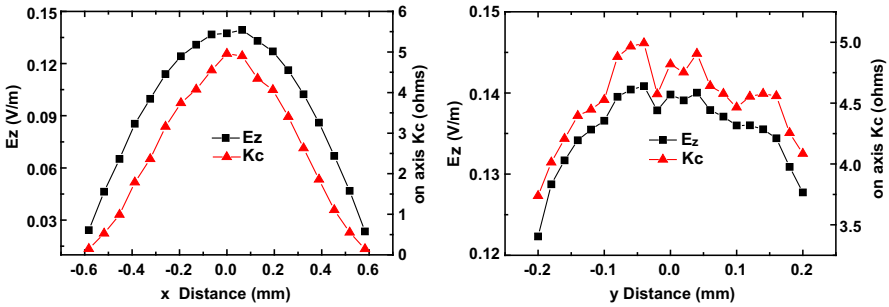

Figure 3. Distribution of electric fields and interaction impedance along the broad wall of (a) the waveguide section and (b) the narrow direction at 140 GHz without the effect of the rectangular beam tunnel.

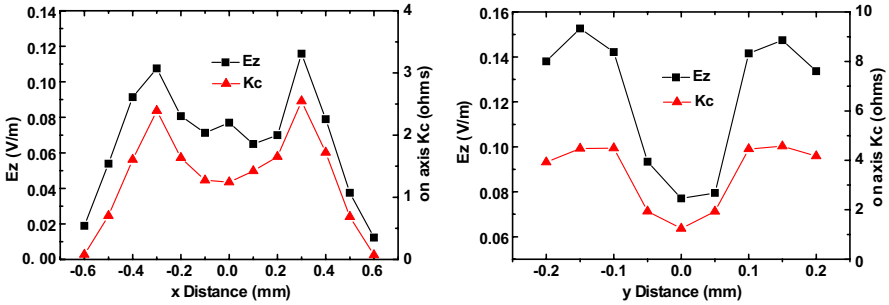

Figure 4. Distribution of electric fields and interaction impedance along the broad wall of (a) the waveguide section and (b) the narrow direction at 140 GHz consideration the effect of the rectangular beam tunnel.

and 0.15 mm along x-direction and y-direction, respectively. It is noted from the Figure 4 that the rectangular beam tunnel could cover almost all the regions of relatively large electric fields around the middle of the waveguide.

3. RADIO-FREQUENCY CHARACTERISTICS

Since the slow-wave structure is periodic, the simulation can be carried out only in one pitch. The high frequency properties of this structure were calculated by the equivalent circuit method which is developed to analyze dispersion characteristics and interaction impedance of the FWG-SWS by our group [12, 18, 19]. For comparison, we also simulated the structure using a 3-D electromagnetic code, HSSS [20]. The dispersion relation and interaction impedance characteristics of the double-ridge loaded FWG-SWS have been plotted in Figure 5. It is observed that there is fairly good agreement between the two methods and that the wave velocity changes slowly when the frequency is varied, which means a very wide bandwidth.

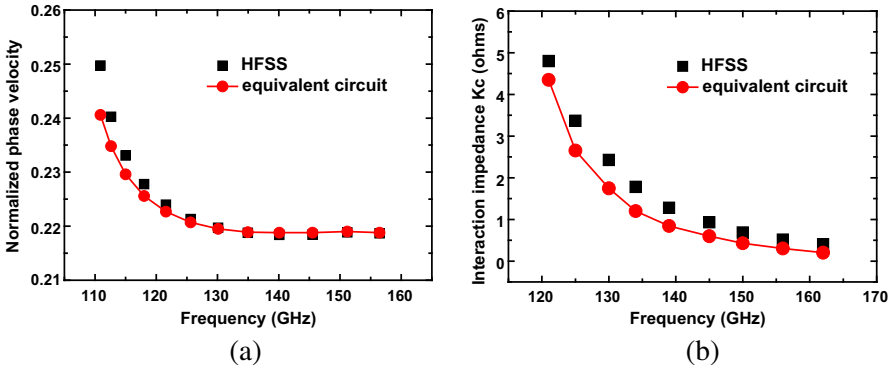

Figure 5. (a) Dispersion curve and (b) interaction impedance of the fundamental mode under the -1 spatial harmonic of the double-ridge loaded FWG-SWS.

4. TRANSMISSION PROPERTY

The signal transmission property of twenty-period double-ridge FWG-SWS with rectangular beam tunnel is presented with the CST transient solver, as shown in Figure 6. It is observed that the reflection parameter S_{11} is almost below -15 dB and that transmission coefficient S_{21} keeps above -0.33 dB through out the bandwidth of 125–160 GHz. In addition, $S_{11} < -20$ dB and $S_{21} > -0.18$ dB from 138 GHz

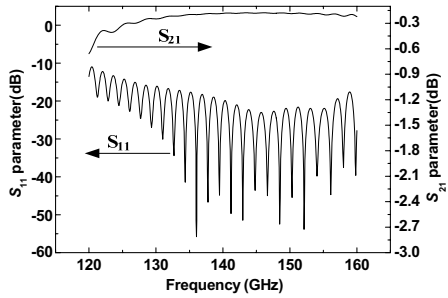

Figure 6. Transmission characteristics of double-ridge loaded slow wave circuit.

to 156 GHz frequency range. This result implies that this circuit structure possesses quite wide bandwidth and low reflection. It is noted that in all simulation of this paper, the material is set as copper with the effective conductivity of 2.2×10^7 S/m considering surface roughness [21].

5. PARTICLE-IN-CELL SIMULATIONS

In this section, a full-scale 3-D circuit model for the double-ridge loaded FWG-TWT is presented. And the CST-PS particle-in-cell code is carried out to investigate the amplification performance of this kind of TWT the model. The dimensional parameters are listed in Table 1. In order to obtain a large gain and suppress the oscillation caused by reflection, the whole interaction circuit is divided into two sections by attenuators shown in Figure 7. The first section consists of 25 periods, and the second section consists of 46 periods.

Table 1. The optimized structural parameters.

Parameters	Value
Waveguide broad wall (a)	1.66 mm
Narrow dimension of the waveguide (b)	0.31 mm
The length of the straight waveguide (h)	0.44 mm
The length of the pitch of the SWS (p)	0.38 mm
The broad wall of the sheet beam tunnel (a_2)	0.54 mm
The narrow dimension of the sheet beam tunnel (b_2)	0.22 mm
Thickness of the ridge (w)	0.062 mm
Height of the ridge (h)	0.44 mm
Thickness of the vane (e)	0.183 mm
Height of the vane (h_1)	0.308 mm

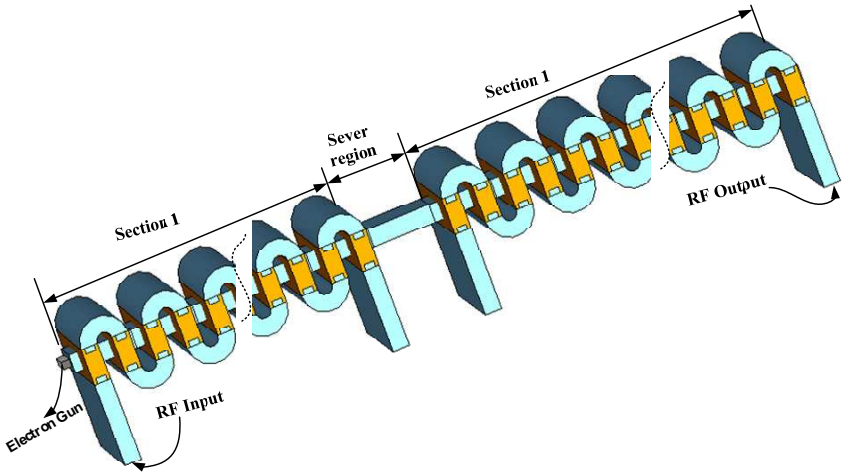

Figure 7. Three-dimensional model of the complete tube of the double-ridge loaded FWG-TWT.

The sever region represents an ideal attenuator and cuts off the propagation path of the signal wave without reflection which includes 3 periods. The beam voltage was held set at an optimized constant value of 12.7 kV. The beam current should be high enough to enhance the efficiency of beam-wave interaction, but low current density is expected, because a space margin between the beam fringe and the tunnel wall is required. Its dimension should be sufficient to reduce the beam focusing requirements. It is assumed that the sheet beam with a current of 150 mA moves through a rectangular cross section of $0.32 \times 0.13\,\text{mm}^2$ in the central area of the beam tunnel corresponding to the beam filling factor is 35% with a current density of $360\,\text{A/cm}^2$. And a uniform magnetic field with amplitude of 0.3 Tesla is used here to confine focus on the electron beam. In our simulations, the driven power is set to 90 mw.

The amplified performance of double-ridge FWG-TWT at 140 GHz was verified. We selected 7 typical frequencies for the calculations to verify the amplitude-frequency response. The results are shown by plotting the output power versus the driving frequencies sweeping from 125 to 155 GHz, as shown in Figure 8(a), where the corresponding gain is also given. As can be seen, the power saturates at 225 W corresponding to the maximum gain 34 dB and beam-wave interaction efficiency 12% at 140 GHz. The maximum output power reaches 342 W at 145 GHz, which corresponds to a gain of 35.8 dB and an interaction efficiency of 18%.

For comparison, we also studied the amplified performance of double-ridge FWG-TWT with a pencil beam at 140 GHz. It is assumed

that the pencil beam with a current of 150 mA moves through a round cross section of $0.1 \times 0.1\,\mathrm{mm}^2$ in the central area of the beam tunnel corresponding to the beam filling factor is 60%. Figure 8(b) shows that amplified power saturates at 43 W corresponding to the beam-wave energy conversion efficiency 3.1%. This means that the novel double-ridge loaded FWG-TWT with sheet beam can obtain higher power and efficiency.

Figure 9 gives the frequency spectrum of input and output signals. As can be seen, the amplified output signal peak is at 140 GHz, and its amplitude is 32 dB higher than the input signal. It is also observed that the higher harmonics of the operating frequency are excited at around 280 GHz and 420 GHz or higher frequencies, but the amplitudes of these higher harmonics are much lower than that of the operating frequency.

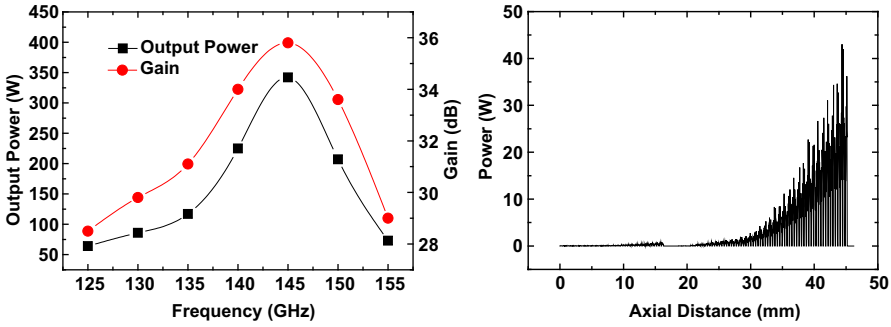

Figure 8. (a) Output power and total gain versus frequency of the double-ridge loaded FWG-TWT with sheet beam and (b) axial power distribution of the double-ridge loaded FWG-TWT with pencil beam.

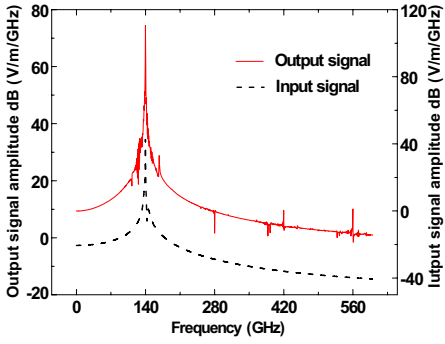

Figure 9. Frequency spectrum of input and output signals for 140 GHz.

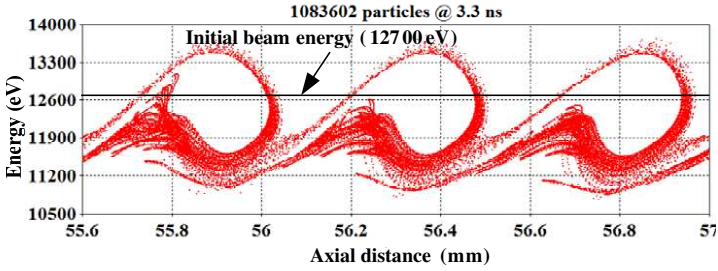

Figure 10. Energy phase space distribution of the particles at the end of the circuit.

Figure 10 shows an enlarged image of the energy distribution of the particles in the phase space along the axial direction at 3.3 ns when the electron dynamic is in a steady state. It is clearly illustrated that the number of the retarded electrons is much more than the accelerated electrons, which means that most electrons transfer their energy to electromagnetic fields and that only a small number of electrons absorb the energy from the electromagnetic fields. Therefore, the output signal has been amplified.

6. SUMMARY AND CONCLUSION

This paper has presented a novel double-ridge loaded FWG-SWS with a sheet beam electron as the RF circuit for TWT operating in the 140 GHz. The electromagnetic properties were calculated by means of the equivalent circuit method. Subsequently, according to the parameters given by the theatrical analysis, the nonlinear interaction of this kind of TWT was investigated. Compared with the traditional FWG-TWT, the novel FWG-TWT with sheet beam has the advantage of higher efficiency and bigger output power. It is revealed that we will provide a new potential of double-ridge loaded FWG-SWS for obtaining high power radiation source at the terahertz frequency. Future work will be concentrated on the practical application of this kind of TWT.

ACKNOWLEDGMENT

This work was supported by the National Science Fund for Distinguished Young Scholars of China (Grant No. 61125103), the National Natural Science Foundation of China (Grant Nos. 60971038 and 60971031), the Fundamental Research Funds for the Central

Universities, China (Grant Nos. ZYGX2010J054 and ZYGX2011J035) and the Fundamental Research Funds of the China West Normal University (Grant Nos. 07B066).

REFERENCES

1. Döhler, G., D. Gagne, D. Gallagher, and R. Moats, "Serpentine wave-guide TWT," *1987 International Electron Devices Meeting*, Vol. 33, 1987.
2. Na, Y. H., S. W. Chung, and J. J. Choi, "Analysis of a broadband Q band folded waveguide traveling-wave tube," *IEEE Trans. on Plasma Sci.*, Vol. 30, No. 3, 1017–1023, Jun. 2002.
3. Gallagher, D., J. Richards, and C. Armstrong, "Millimeter-wave folded waveguide TWT development at Northrop Grumman," *IEEE International Conference on Plasma Science*, Vol. 161, 1997.
4. Gallagher, D., J. Tucek, M. Converse, et al., "Optimized design of folded waveguide TWTs," *Proc. Int. Vac. Electron. Conf.*, Vol. 46, 2002.
5. Booske, J. H., "New opportunities in vacuum electronics through the application of microfabrication technologies," *Proc. Int. Vac. Electron. Conf.*, 11–12, Apr. 2002.
6. Alan, J. T., C. J. Meadows, and R. B. True, "Experimental investigation of a novel circuit for millimeter-wave TWTs," *IEEE Trans. on Electron Devices*, Vol. 54, No. 5, 1054–1060, 2007.
7. Bhattacharjee, S., J. H. Booske, C. L. Kory, D. W. van der Weide, S. Limbach, S. Gallagher, J. D. Welter, M. R. Lopez, R. M. Gilgenbach, R. L. Ives, M. E. Read, R. Divan, and D. C. Mancini, "Folded waveguidetraveling-wave tube sources for terahertz radiation," *IEEE Trans. on Plasma Sci.*, Vol. 32, No. 3, 1002–1014, Jun. 2004.
8. Booske, J. H., M. C. Converse, C. L. Kory, C. T. Chevalier, D. A. Gallagher, K. E. Kreischer, V. O. Heinen, and S. Bhattacharjee, "Accurate parametric modeling of folded waveguide circuits for millimeter-wave traveling wave tubes," *IEEE Trans. on Electron Devices*, Vol. 52, No. 5, 685–694, May 2005.
9. Han, S. T., J. I. Kim, K. H. Jang, J. K. So, S. S. Chang, N. M. Ryskin, and G. S. Park, "Experimental investigation of millimeter wave folded-waveguide TWT," *Proc. Int. Vac. Electron. Conf.*, 322–323, May 2003.
10. Kory, C., J. David, H. T. Tran, L. Ives, and D. Chernin, "Folded

waveguide circuit optimizations using Christine 1D," *Proc. 32nd IEEE Int. Conf, Plasma Sci.*, 333, Jun. 2005.

11. Han, S. T., J. I. Kim, and G. S. Park, "Design of a folded waveguide traveling-wave tube," *Microw. Opt. Technol. Lett.*, Vol. 38, No. 2, 161–165, Jul. 2003.
12. Hou, Y., Y. B. Gong, J. Xu, S. M. Wang, et al., "A novel ridge-vane loaded folded waveguide slow-wave structure for 0.22 THz traveling-wave tube," *IEEE Trans. on Electron Devices*, Vol. 60, No. 3, 1228–1235, May 2013.
13. He, J., Y. Y. Wei, Z. G. Lu, et al., "Investigation of a ridge-loaded folded waveguide slow-wave system for the millimeter wave traveling wave tube," *IEEE Trans. on Plasma Sci.*, Vol. 38, No. 7, 1556–1562, 2010.
14. Liu, Y., J. Xu, Y.-Y. Wei, X. Xu, F. Shen, M. Huang, T. Tang, W.-X. Wang, Y.-B. Gong, and J. Feng, "Design of a V-band high-power sheet-beam coupled-cavity traveling-wave tube," *Progress In Electromagnetics Research*, Vol. 123, 31–45, 2012.
15. Duan, Z., Y. Wang, X. Mao, W.-X. Wang, and M. Chen, "Experimental demonstration of double-negative metamaterials partially filled in a circular waveguide," *Progress In Electromagnetics Research*, Vol. 121, 215–224, 2011.
16. Shin, Y. M., L. R. Barnett, A. Baig, N. C. Luhmann, Jr., J. Pasour, and P. Larsen, "Modeling investigation of an ultrawideband terahertz sheet beam traveling-wave tube amplifier circuit," *IEEE Trans. on Electron Devices*, Vol. 58, No. 9, 3213–3218, Sep. 2011.
17. CST Corp., CST PS Tutorials, [Online], available: http://www.cst-china.cn/CST2009.
18. Hou, Y., J. Xu, H.-R. Yin, Y.-Y. Wei, L.-N. Yue, G. Zhao, and Y.-B. Gong, "Equivalent circuit analysis of ridge-loaded folded-waveguide slow-wave structures for millimeter-wave traveling-wave tubes," *Progress In Electromagnetics Research*, Vol. 129, 215–229, 2012.
19. Liu, S., "Folded waveguide circuit for broadband MM wave TWTs," *Int. J. Infrared Millim Waves*, Vol. 16, 809–815, 1995.
20. Ansoft Corp., Ansoft HFSS User's Reference, [Online], available: http://www.ansoft.com.cn/.
21. Kory, C., et al., "Overview of W-band traveling wave tube programs," *IEEE International Vacuum Electronics Conference, 2006 Held Jointly with 2006 IEEE International Vacuum Electron Sources.*, 447–448, 2006.